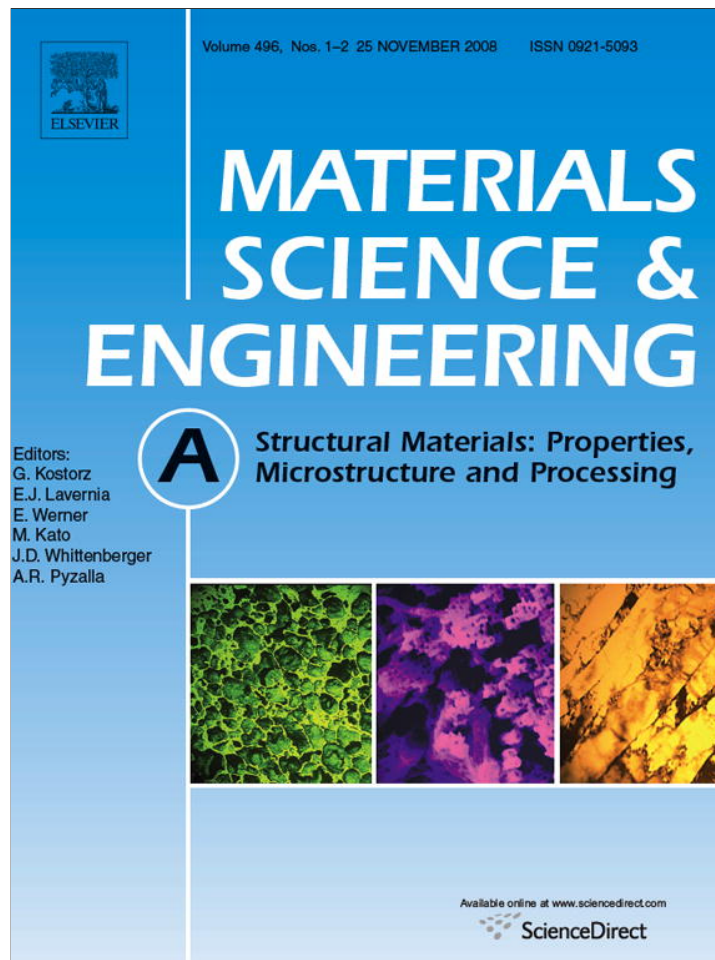


Provided for non-commercial research and education use.
Not for reproduction, distribution or commercial use.



This article appeared in a journal published by Elsevier. The attached copy is furnished to the author for internal non-commercial research and education use, including for instruction at the authors institution and sharing with colleagues.

Other uses, including reproduction and distribution, or selling or licensing copies, or posting to personal, institutional or third party websites are prohibited.

In most cases authors are permitted to post their version of the article (e.g. in Word or Tex form) to their personal website or institutional repository. Authors requiring further information regarding Elsevier's archiving and manuscript policies are encouraged to visit:

<http://www.elsevier.com/copyright>



Contents lists available at ScienceDirect

Materials Science and Engineering A

journal homepage: www.elsevier.com/locate/msea

Tensile and compressive deformation behaviors of commercially pure Al processed by equal-channel angular pressing with different dies

J.W. Wang, Q.Q. Duan, C.X. Huang, S.D. Wu, Z.F. Zhang*

Shenyang National Laboratory for Materials Science, Institute of Metal Research, Chinese Academy of Science, Shenyang 110016, PR China

ARTICLE INFO

Article history:

Received 31 March 2008

Received in revised form 23 May 2008

Accepted 26 May 2008

Keywords:

Commercially pure Al

Equal-channel angular pressing

Tension

Compression

Strength

Shear bands

ABSTRACT

An investigation was conducted on the tensile and compressive properties of commercially pure Al processed by equal-channel angular pressing (ECAP) with two different dies. The specimens along two different directions were cut from the ECAPed billets to study the effect of orientation on the compressive yield strength and the surface deformation morphologies along normal direction (ND) and extrusion direction (ED). It was found that the yield strength of the specimens along ED under tension was lower than that along ED under compression, but higher than that along ND under compression. The surface observations showed that there were some differences in the deformation morphologies under compression along two different directions. Based on the mechanical tests and observations of surface morphologies of ECAPed pure Al, the relationship between shear deformation behavior and tension/compression asymmetry was discussed.

© 2008 Elsevier B.V. All rights reserved.

1. Introduction

In the past decade, the technique of equal-channel angular pressing (ECAP) has attracted much attention as a method of severe plastic deformation (SPD) to produce ultrafine-grained (UFG) or submicron-grained (SMG) materials [1–6]. Up to now, many metals and alloys have been fabricated into UFG materials with high strength or superplasticity via ECAP technique, albeit their ductility is decreased in comparison with that in their coarse-grained counterparts [7–9]. In general, ECAP can apply a high shear strain to materials through a specially designed die having two equally sized channels connected at a finite angle [1,10]. It is noted that the high shear strain often induces shear flow lines or textures in the ECAPed materials [1,11–14], leading to a significant anisotropy in strength [11–13]. Although the mechanical properties of ECAPed materials have been extensively investigated, there are few reports about their anisotropic properties [13].

Tabachnikova et al. [11] studied the tensile and compressive properties of commercially pure Ti and UFG Ti at ambient temperature processed by ECAP, and found that the stress differential (SD) effect values (anisotropic degree in strength) are significantly different for samples strained along the directions parallel and perpendicular to the ECAP axis. Han et al. [12] investigated the

anisotropic compressive properties and shear deformation mechanism of pure iron subjected to ECAP with single-pass, suggesting that the shear plane induced by the first pass of ECAP is a relatively weak plane to resist subsequent shear deformation. In addition, the effects of strain path on the flow stress anisotropy and Bauschinger effect (BE) in UFG Cu were investigated by Haouaoui et al. [13]. They found that the SD ratio was always negative along the extrusion direction, regardless of the route and number of ECAP pass. They argued that the change of SD ratio could be affected not only by the crystallographic texture and grain size but also by the grain morphology and grain boundary characters. Recently, Yu et al. [14] reported that the yield strength under compression was about 20% higher than that under tension for SMG Al processed by ECAP over a grain size range of 350–750 nm, which disappeared for their counterparts with larger grain size. For ECAPed materials, the plastic deformation often localizes into some shear bands [1,15]. The shear localization was observed in compression tests in ECAPed samples [14], but the strength asymmetry between tension and compression in ECAPed Al and its alloys has not been paid much attention to establish the relationship between the shear localization and strength asymmetry. In particular, most researches ignored the differences in the shear deformation behaviors on the specimens compressed along different directions [11,13].

In general, most ECAP process are conducted using a die angle of 90°, applying the equivalent strain of about 1 per pass [16]. But some researches have also performed ECAP tests in the dies having different channel angles in order to reveal its deformation

* Corresponding author. Tel.: +86 24 23971043.

E-mail address: zhfzhang@imr.ac.cn (Z.F. Zhang).

mechanism. Furukawa et al. [6] studied the shearing patterns during ECAP under three different routes using die angles of 90° and 120° , respectively, and discussed the microstructure evolution in different routes. Furuno et al. [17] observed the microstructures and texture of the ECAPed pure Al and Al–1%Mg–0.2%Sc alloy with a die having an internal channel angle of 60° . In addition, Zheng et al. [18] investigated the structure and mechanical properties of 7050 and 2224 Al alloys with ultrafine grains produced by ECAP using a die angle of 120° . Though pure Al has been studied by many researchers as a model material to reveal the deformation mechanism of ECAP in dies having different channel angles, the anisotropic properties and the strength asymmetry under tensile and compressive loading have not been systematically investigated for pure Al processed by ECAP using dies with different channel angles. In the present work, we studied the mechanical properties of commercially pure Al processed by ECAP for one or two passes using dies with 90° and 120° channel angles, respectively. The strength asymmetry under tension and compression is discussed in terms of their surface deformation morphologies.

2. Experimental procedure

The experimental material in the present work is 1060 commercially pure Al. Firstly, the Al plate was annealed at 390°C for 0.5 h, gaining the average grain size of about $20\ \mu\text{m}$. Secondly, the plate was made into some billets with a dimension of $8\ \text{mm} \times 8\ \text{mm} \times 70\ \text{mm}$ by spark cutting technique. Then, ECAP was conducted at room temperature (RT) to extrude the Al billets using two kinds of dies having different intersecting channel angles, which one is $\Phi = 90^\circ$ and $\Psi = 90^\circ$ and the other is $\Phi = 120^\circ$ and $\Psi = 0^\circ$. The estimated equivalent strain applied in each pass is 0.91 for the 90° die, and 0.67 for the 120° die, respectively [3]. Fig. 1 demonstrates the schematic drawing of the ECAP die, where three perpendicular directions are defined as extrusion direction (ED), transverse direction (TD) and normal direction (ND).

The samples were subjected to ECA pressing for one or two passes in the 90° die. Between the two passes, the samples were rotated by 90° around ED. But the samples were only extruded for one pass in the 120° die. Before pressing, the billets were coated with MoS_2 as lubricant. After ECAP, some tensile specimens with cross-section of $1.5\ \text{mm} \times 2\ \text{mm}$ and gauge length of 8 mm were machined from the ECAPed samples with their tensile axes parallel to the ED, as shown in Fig. 2. Then, some compressive specimens with a dimension of $3\ \text{mm} \times 3\ \text{mm} \times 6\ \text{mm}$ were cut from the extruded billets. Fig. 2 illustrates the compressive specimens having different orientations with respect to the ED. Tensile and compressive specimens were then mechanically grounded by using abrasive papers and finally electro-polished in a solution of 20% per-

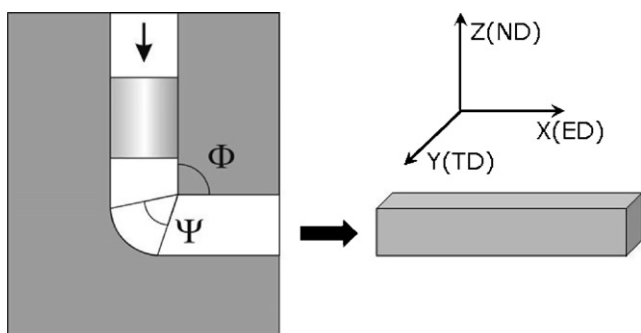


Fig. 1. Illustration of ECAP die and the definitions of ND, ED and TD, respectively.

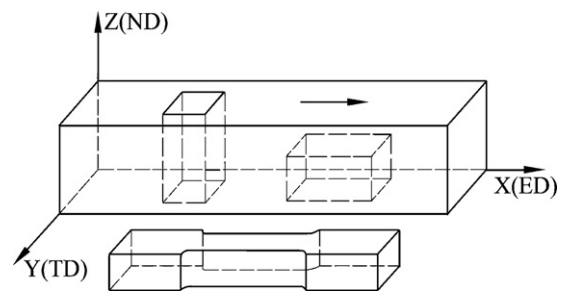


Fig. 2. Illustration of tensile and compressive specimens with the ECAPed billet.

chloric acid and 80% alcohol. Tensile and compressive experiments were conducted at room temperature using Instron 8871 testing machine operated at a constant rate of cross-head displacement with a strain rate of about $5 \times 10^{-4}\ \text{s}^{-1}$. Three tensile experiments were conducted to check the repeatability of the results up to fracture. Two compressive specimens were performed under each condition: one sample was compressed to an engineering strain of about 10% for the observation of surface deformation morphologies, while the other was compressed to an engineering strain more than 25%.

After tension or compression tests, surface deformation morphologies and fractographies were observed using a LEO Supra 35 scanning electron microscope (SEM), as well as Quanta 600 SEM. The microstructure of the ECAPed samples were examined by a JEM-2000FX II transmission electron microscope (TEM). Specimens for TEM observations were cut from the center of the ECAPed billets parallel to the Y-plane, mechanically grounded to about $50\ \mu\text{m}$ and finally thinned by twin-jet electro-polishing method with a solution of 25% nitric acid–methanol. The TEM observation shows that the grains were elongated along the ECAP shear direction and there are many elongated dislocation cells. The statistics analysis shows that the average width of the elongated grains is about $1\text{--}2\ \mu\text{m}$ after two ECAP passes, and the length of the grains is in the range of $2\text{--}3\ \mu\text{m}$.

3. Results and discussion

3.1. Tensile deformation and fracture behaviors

The tensile stress–strain curves of commercially pure Al before and after ECAP are shown in Fig. 3. Fig. 3(a) demonstrates that commercially pure Al has been significantly strengthened after ECAP, but its elongation decreases drastically. For example, its yield strength is more than doubled after extrusion only for one pass, from 41 to 108 MPa, but the uniform elongation decreases from about 40% to less than 3%. After ECAP for two passes, the increase in strength is less significant, indicating that there is slight strain hardening similar to that of most ECAPed materials [19].

Fig. 3(b) presents the tensile stress–strain curves of commercially pure Al extruded only for one pass with two different dies. It is noted that the strength of the specimens conducted through 120° die is always lower than that conducted through the 90° die because the strain applied to the extruded sample in the 120° die is lower than that of the 90° die. In addition, it should be pointed out that the tensile properties of the specimens extruded by the 120° die have more scatter than those of the 90° die, as shown in Fig. 3(b). Wu and Baker [15] have simulated the shear deformation processes using plasticine and concluded that the die with a lower Ψ value will result in more non-uniform deformation than that with a higher one. In present work, the Ψ value of the 120° die is 0° , which will introduce more non-uniform deformation during

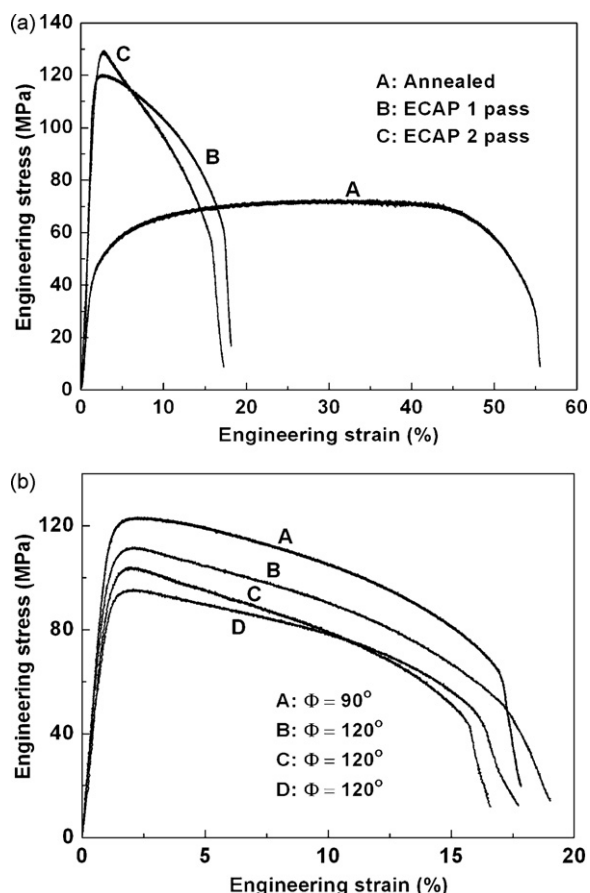


Fig. 3. Tensile stress–strain curves of commercially pure aluminum before and after ECAP. (a) Tensile stress–strain curves of specimens after ECAP for one and two passes by 90° die and (b) comparison of tensile stress–strain curves after ECAP for one pass using different dies.

the ECAP process, making the tensile properties of different samples more scatter.

Fig. 4 shows the fractographies of tensile specimens before and after ECAP. All the tensile specimens display obvious necking, and some slip bands appear on the surface of tensile specimens. It is noted that the uniform elongation of ECAPed specimens is very low, which leads to immediate necking after very little work hardening in tension. In addition, it is found that there are a large number of equiaxial dimples in the fracture zone for all the specimens, indicating a typical ductile fracture. At the bottom of the dimples, there are small holes, which are the initiation sites for fracture [20]. The holes were probably induced by impurities. The average densities of the holes were measured and seem to be approximately the same (about 6×10^4 to 7×10^4 per mm^2) before and after ECAP. The reason might be that the densities of the impurities are also the same [20].

With the ECAP pass increasing, the distribution of dimples has slightly changed. For the annealed specimens, the dimples in the fracture zone are mainly large and deep, as shown in Fig. 4(a). Between the large ones, there are also some small and shallow dimples. When the samples were extruded for one pass, the dimples become shallow and distribute more uniformly, as shown in Fig. 4(b). After ECAP for two passes, there are few large dimples and nearly all the dimples become very small and shallow, as shown in Fig. 4(c). This indicates that the size and distribution of dimples on tensile fracture surfaces are also dependent on the number of ECAP pass. It is known that the ductility of material was signifi-

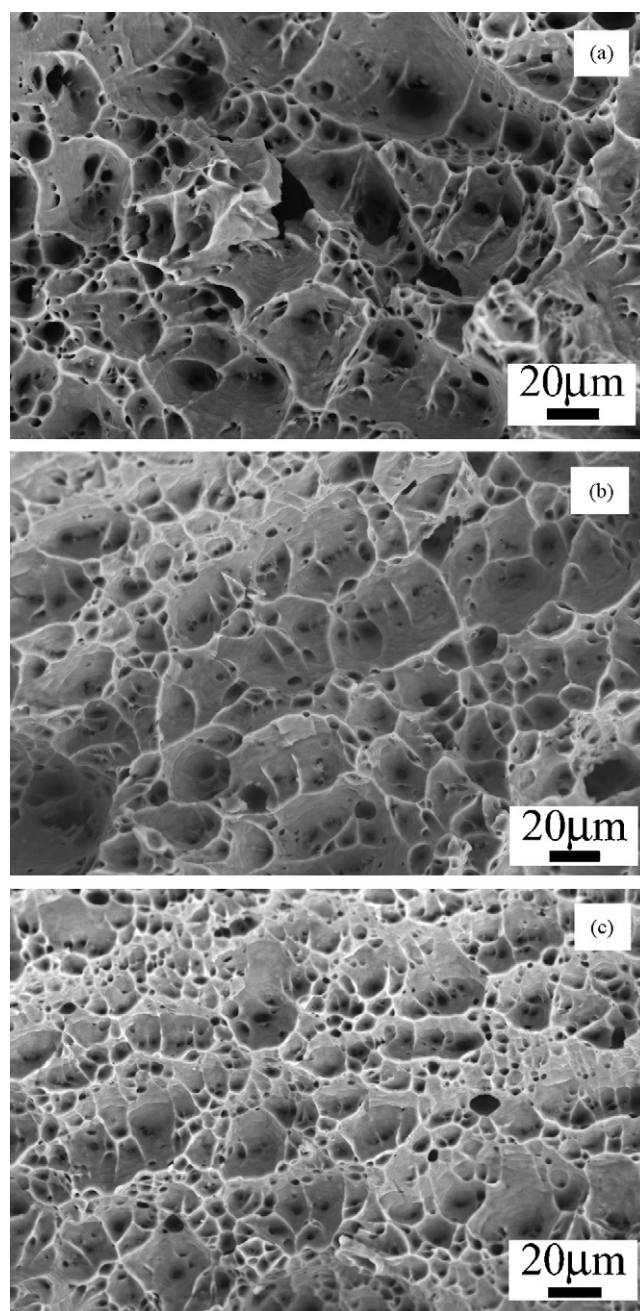


Fig. 4. The tensile fractographies of commercially pure aluminum before and after ECAP: (a) annealed, (b) ECAPed for one pass and (c) ECAPed for two passes.

cantly decreased after ECAP and the uniform elongation becomes very low, indicating a great loss in the work hardening ability. Once the dimples nucleated, there is not enough time to grow and assemble with other dimples around it, inducing shallower dimples. In addition, according to the results of previous researches [20–23], the decrease in the dimple size should be associated with the grain refinement of samples processed by ECAP. It is known that after ECAP for one pass, the grains were elongated along a direction about 27° with respect to the tensile axis [13,24]. Although the grains cannot be refined to a fine level along its length direction after one or two ECAP passes, the average width should be smaller [13], which should affect the dimple size. The smaller the width of the grains is, the smaller the dimples on the tensile fracture are.

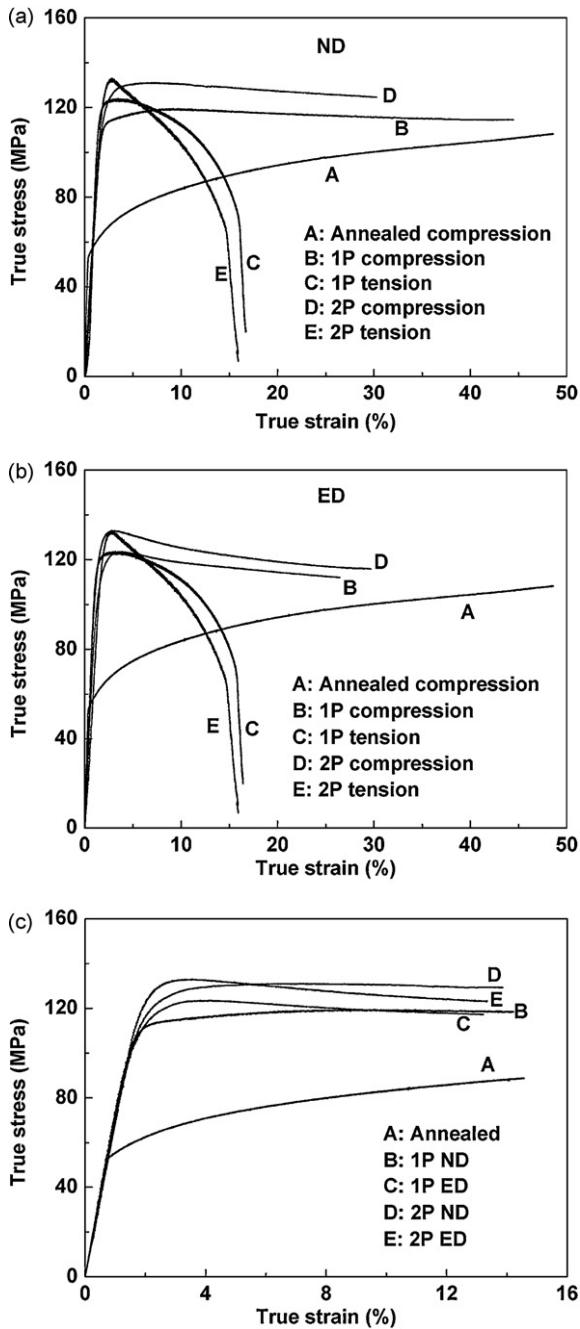


Fig. 5. Comparison of tensile and compressive true stress–strain curves of the specimens along (a) ND and (b) ED. (c) Comparison of compressive true stress–strain curves of the specimens along different directions.

3.2. Compressive behavior

The asymmetry of plastic deformation in ECAPed materials has been proved by many researches [11–14]. Fig. 5 shows the true stress–strain curves of specimens along different directions before and after ECAP under tension and compression. When compressing along ND, the ECAPed specimens show practically no work hardening after yielding when the applied strain is low, and the specimens show slightly softening with the strain increasing, as shown in Fig. 5(a) and (c). Fig. 5(b) shows the true stress–strain curves of the specimens along the ED under compression. It can be seen that there is an obvious strain softening in the stress–strain curves of

the ECAPed specimens after yielding, which is different from that along the ND. With the compressive strain increasing, compressive stress along the ED will continue to decrease, making the specimens softening. The true stress–strain curves along the ND and ED under compression are presented in Fig. 5(c) for comparison. It is noted that the strain softening rate along the ED under compression seems to be higher than that along the ND no matter whether for the samples extruded for one or two passes. In addition, the compressive yield strength along the ED is higher than that along the ND, which is well consistent with the result of AISI 304L stainless steel under compression [25].

When compressing along different directions, the surface deformation morphologies display quite different features, as shown in Fig. 6. The surface of the annealed specimen has very dense multiple slip bands in the interior of coarse grains, as shown in Fig. 6(a) and (b). After ECAP, the plastic strains mainly localized in shear bands, as shown in Fig. 6(c)–(f). On the other hand, there are also some slip bands on the specimen surface after ECAP for one pass, but with low density compared with that of the annealed specimen, as shown in Fig. 6(a) and (c). In addition, with the accumulation of compressive strain, some shear bands will develop to form the highly plastic strain localization zone, and they are small and discontinuous when the strain is low. With further increase in the accumulation of compressive strain, more and more shear bands will evolve and link each other. After ECAP for two passes, the shear bands become more straight and dense and only few slip bands can be seen on the specimen surface, as shown in Fig. 6(e) and (f).

The surface topographies of specimens under compression along the ED are very different from that along the ND, as shown in Fig. 7. It seems that the plastic strain is mainly localized within the slip bands on the specimen surface when pressing along the ED, but the shear bands become not obvious. When the specimen was pressed for one pass, the localized shear bands and slip bands only formed and developed along one direction, as shown in Fig. 7(a) and (b). However, the dense slip bands along two directions arise to form a cross-weaved structure when specimen was subjected to two passes, as shown in Fig. 7(c) and (d). One group of slip bands is very strong, and the other is relatively weak.

It is well known that dislocations were piled-up at the boundaries of the elongated grains after ECAP [13,26–28]. Fig. 8(a) illustrates the distribution of dislocations in the elongated grains after ECAP for one pass. In addition, the normal and shear stresses conducted on the ECAP shear plane for one-pass pressing under tension and compression are demonstrated in Fig. 8(b)–(d). The normal stress σ and shear stress τ acted on the ECAP shear plane can be expressed as [29]:

$$\sigma_{\theta} = \sigma \sin^2 \theta \quad (1)$$

$$\tau = \sigma \sin \theta \cos \theta \quad (2)$$

where, σ is the applied stress under tension or compression and θ is the angle between the ECAP shear plane and the loading direction. For the compression specimens along the ND and ED, the angles θ are approximately equal to 63° and 27° , respectively. It is known that a large shear strain has been conducted and the grains were elongated along the ECAP shear direction in the ECAP process [30,31]. When dislocations move along the ECAP shear direction, it will have a larger free slip distance for dislocations than along other directions [12]. With more and more dislocations slipping along this direction and terminate at grain boundaries, the dislocations are piled-up along this direction near the elongated grain boundaries [13,28], as illustrated in Fig. 8(a). Then, it is difficult to move for dislocations under the subsequent stress conducted along the same direction, which makes further deformation more difficult. Under tension, the direction of shear stress τ conducted

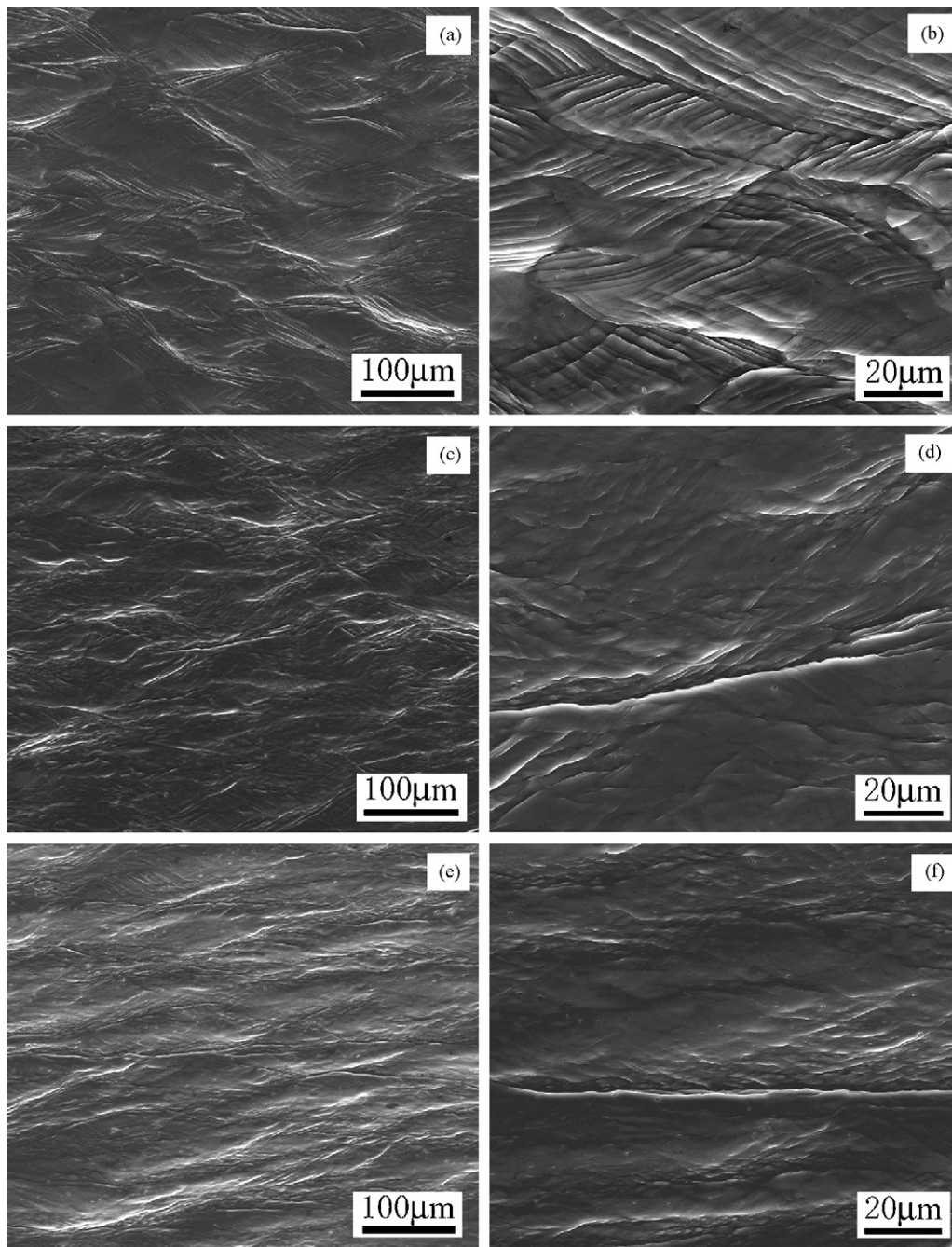


Fig. 6. The surface deformation morphologies of compressive specimens along ND. (a) and (b) annealed specimens; (c) and (d) ECAPed specimens for one pass; (e) and (f) ECAPed specimens for two passes.

on the ECAP shear plane is identical to the ECAP shear direction, as illustrated in Fig. 8(b). It will be very difficult for dislocations to slip along this direction, behaving in a lower strain hardening before necking [27,32], as shown in Fig. 3. Therefore, the low strain hardening should be associated with the dislocations trapped at the elongated grain boundaries [27].

However, it will produce reverse shear stress τ and normal stress σ on the ECAP shear plane under compressive stress, as shown in Fig. 8(c) and (d). Under the shear stress τ , dislocations can continually slip along the opposite direction of the ECAP shear direction and be annihilated [11,13], as illustrated in Fig. 8(c) and (d), resulting in an asymmetry of the strength. When compression is conducted on specimens along the ND, the normal stress σ acted on the ECAP

shear plane is much higher than the shear stress τ under compression along the ND, as shown in Fig. 9. Under the normal stress σ , the ECAP shear plane will rotate around the compressive axis, which will make the shear plane gradually become perpendicular to the compressive axis [33]. In this process, it is accompanied by the geometric hardening and softening of material [33]. The competition of hardening and softening induces very little work hardening when the applied strain is low, as shown in Fig. 5(c). Under compression, it can also be extruded along the shear plane in the strain localization zone, which will develop to severe surface shear bands even cracking with the compressive strain accumulation, as shown in Fig. 6. When compressing along the ED, the shear stress on the ECAP shear plane is a little bit larger than the normal stress, as illus-

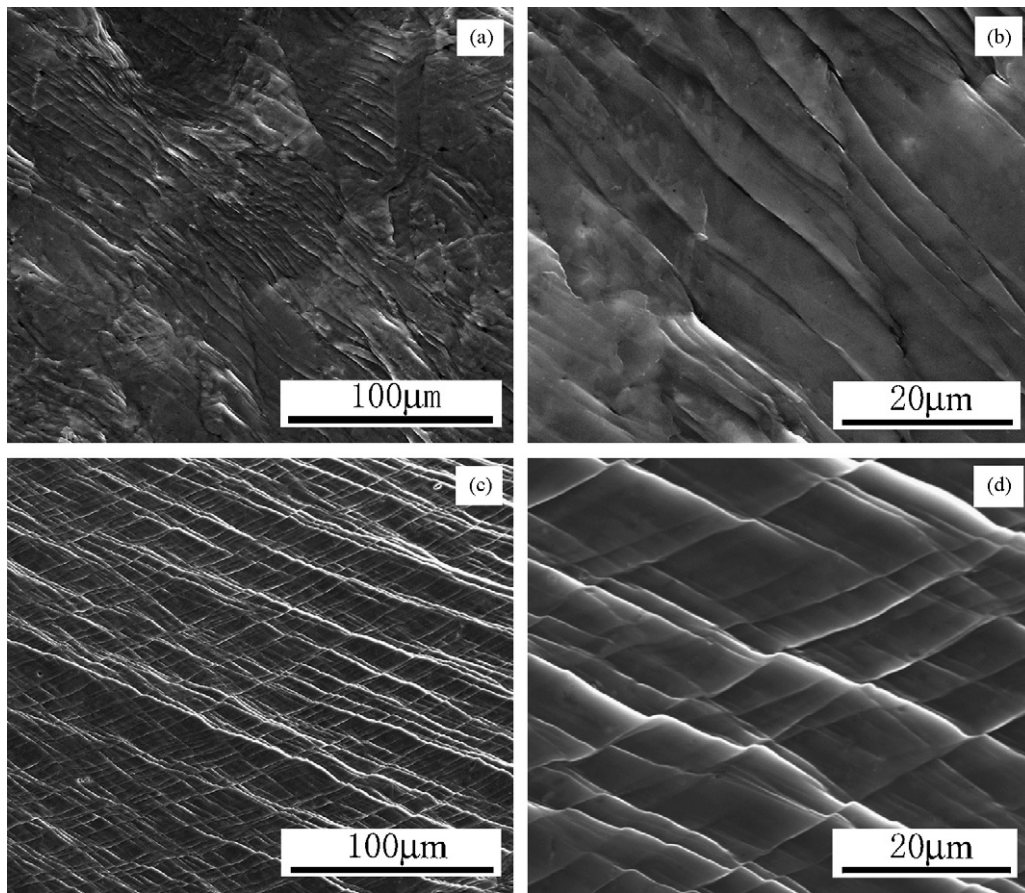


Fig. 7. The surface deformation morphologies of compressive specimens along ED. (a) and (b) ECAPed specimens for one pass; (c) and (d) ECAPed specimens for two passes.

trated in Fig. 9. Under the shear stress τ , dislocations can easily slip along the opposite direction of the ECAP shear direction, inducing positive geometric softening, as illustrated in Fig. 5(b) and Fig. 8(d). In addition, the higher shear stress along the ECAP shear plane will induce dense slip bands on the specimen surface, as shown in Fig. 7.

3.3. Strength asymmetry under tension and compression

The dependence of yield strength under tension and compression on the number of ECAP passes is shown in Fig. 10. It can be seen that the specimens without ECAP have identical tensile and compressive strength, indicating a good isotropic property. However, with increasing the number of ECAP pass, the yield strength in both

tension and compression has a great increase. Comparing the yield strength under tension and compression, it is found that the yield strength along the ED under tension is lower than that along the ED under compression, but higher than that along the ND under compression, as shown in Fig. 10. The yield strength asymmetry under tension and compression along different directions might be associated with texture. It has been revealed that a B-type rolling texture could be formed in an aluminum single crystal after ECAP only for one pass by Fukuda et al. using a 90° die [34]. However, the grain morphology and grain boundaries may also affect the strength asymmetry [13].

The asymmetry of plastic deformation of crystalline materials widely consists in the difference in their mechanical properties

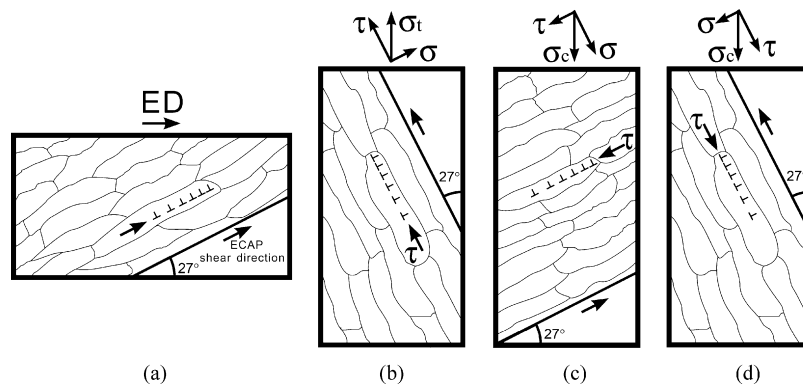


Fig. 8. The illustration of dislocation distribution in the elongated grains for the specimens ECAPed for one pass and the shear stress conducted on the ECAP shear plane under tension and compression. (a) As ECAPed specimens; (b) tension and (c) compression along ND; (d) compression along ED.

Table 1
Stress differential values along different directions before and after ECAP

Number of ECAP pass	$\sigma_{0.2}^c$ (MPa)	$\sigma_{0.2}^c$ (ND) (MPa)	$\sigma_{0.2}^c$ (ND) (MPa)	Stress difference (SD), Δ (%)	
				ND	ED
Annealed	41	41	41	–	0
1P	108	104	122	–15.9	12.17
2P	119	112	126	–11.8	5.71

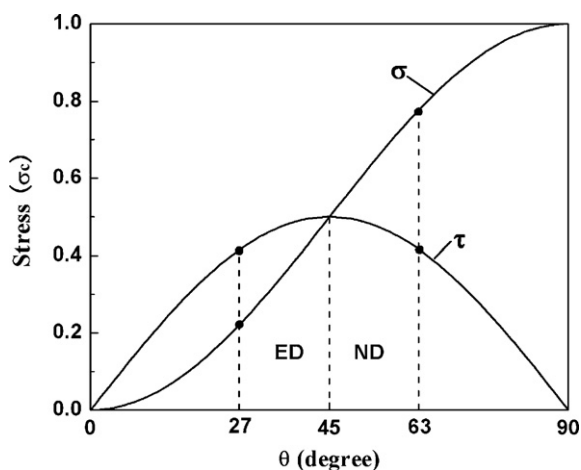


Fig. 9. Distribution of normal and shear stresses on different shear plane.

under uniaxial tension and compression. This phenomenon has been well pronounced during plastic deformation by slip of bcc transition metal single crystals and in a number of polycrystalline metals [11]. It is known that there is a stress differential effect [35], which can be expressed as [11]:

$$\Delta = \frac{\sigma_y^c - \sigma_y^t}{0.5(\sigma_y^c + \sigma_y^t)} \quad (3)$$

where σ_y^t and σ_y^c are yield strengths under tension and compression. The yield strength and SD values were calculated and are listed in Table 1. Since the tensile strength along the ND cannot be tested due to the limitation of the ECAPed billet dimension, the compressive yield strength under different directions were used to calculate the SD values along the ND. It is noted that the SD values along the ED decrease with the increase in the ECAP pass, which means that the

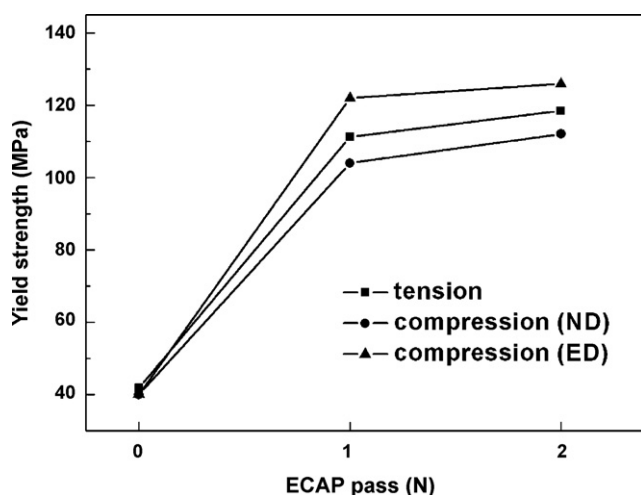


Fig. 10. Dependence of yield strength in tension and compression on the number of ECAP passes.

tension/compression (T/C) asymmetry decreases. In addition, the T/C asymmetry along the ND also decreases with increasing the ECAP pass, as shown in Table 1. The factors responsible for the SD effect have been analyzed by Haouaoui et al. [13]. They argued that not only the crystallographic texture and grain size are the factors affecting the phenomena observed, but also grain morphology and grain boundaries play an important role in the strength asymmetry. On the other hand, the ECAP shear plane should also affect the strength asymmetry under tension and compression [12,25].

4. Conclusions

- (1) The tensile stress–strain curves of the specimens pressed by a 120° die is much scatter than that by a 90° die, which should be highly associated with much non-uniform shear deformation during pressing.
- (2) There are mainly large and deep dimples in the fracture zone of the annealed tensile specimens. With increasing the number of ECAP pass, the amount of small dimples increases, and the dimples become shallow and more uniform.
- (3) When compressing along different directions, the specimens displayed different compressive stress–strain curves and their surface deformation morphologies are also different. The specimens under compression along the ND show practically no strain hardening after yielding when the compressive strain is low and some shear bands formed on the specimen surface. However, there is obvious strain softening after yielding in the compressive stress–strain curves along the ED. With compressive strain increasing, specimens along two directions show continual strain softening.
- (4) The yield strength of the specimens along the ED under tension is lower than that along the ED under compression, but higher than that along the ND under compression. In addition, the T/C asymmetry along both directions decreases with increasing the ECAP pass.

Acknowledgements

The authors would like to thank W. Gao, H.H. Su, G. Yao and M.J. Zhang for the assistance in the sample preparation, mechanical tests, SEM and TEM observations. This work was financially supported by “Hundred of Talents Project” by Chinese Academy of Sciences and the National Outstanding Young Scientist Foundation under Grant No. 50625103.

References

- [1] V.M. Segal, Mater. Sci. Eng. A 197 (1995) 157.
- [2] V.M. Segal, Mater. Sci. Eng. A 271 (1999) 322.
- [3] R.Z. Valiev, T.G. Langdon, Prog. Mater. Sci. 51 (2006) 881.
- [4] R.Z. Valiev, E.V. Kozlov, Y.F. Ivanov, J. Lian, A.A. Nazarov, B. Baudalet, Acta Metall. Mater. 42 (1994) 2467.
- [5] M.A. Muñoz-Morris, C.G. Oca, D.G. Morris, Scripta Mater. 48 (2003) 213.
- [6] M. Furukawa, Z. Horita, T.G. Langdon, Mater. Sci. Eng. A 332 (2002) 97.
- [7] Z.C. Wang, P.B. Prangnell, Mater. Sci. Eng. A 328 (2002) 87.
- [8] W.J. Kim, S.I. Hong, Y.S. Kim, S.H. Min, H.T. Jeong, J.D. Lee, Acta Mater. 51 (2003) 3293.
- [9] T.L. Tsai, P.L. Sun, P.W. Kao, C.P. Chang, Mater. Sci. Eng. A 342 (2003) 144.
- [10] T. Aida, K. Matsuki, Z. Horita, T.G. Langdon, Scripta Mater. 44 (2001) 575.

- [11] E.D. Tabachnikova, V.Z. Bengus, V.V. Stolyarov, G.I. Raab, R.Z. Valiev, K. Csach, J. Miskuf, Mater. Sci. Eng. A 309–310 (2001) 524.
- [12] W.Z. Han, Z.F. Zhang, S.D. Wu, S.X. Li, Y.D. Wang, Philos. Mag. Lett. 86 (2006) 435.
- [13] M. Haouaoui, I. Karaman, H.J. Maier, Acta Mater. 54 (2006) 5477.
- [14] C.Y. Yu, P.L. Sun, P.W. Kao, C.P. Chang, Scripta Mater. 52 (2005) 359.
- [15] Y. Wu, I. Baker, Scripta Mater. 35 (1997) 437.
- [16] Y. Iwahashi, J.T. Wang, Z.J. Horita, M. Nemoto, T.G. Langdon, Scripta Mater. 35 (1996) 143.
- [17] K. Furuno, H. Akamatsu, K. Oh-ishi, M. Furukawa, Z. Horita, T.G. Langdon, Acta Mater. 52 (2004) 2497.
- [18] L.J. Zheng, C.Q. Chen, T.T. Zhou, P.Y. Liu, M.G. Zeng, Mater. Charact. 49 (2003) 455.
- [19] R.Z. Valiev, Mater. Sci. Eng. A 234 (1997) 59.
- [20] A. Mishra, B.K. Kad, F. Gregori, M.A. Meyers, Acta Mater. 55 (2007) 13.
- [21] A. Vinogradov, T. Ishida, K. Kitagawa, V.I. Kopylov, Acta Mater. 53 (2005) 2181.
- [22] D.R. Fang, Q.Q. Duan, N.Q. Zhao, J.J. Li, S.D. Wu, Z.F. Zhang, Mater. Sci. Eng. A 459 (2007) 137.
- [23] S.K. Panigrahi, R. Jayaganthan, Mater. Sci. Eng. A, in press.
- [24] K. Kamachi, M. Furukawa, Z. Horita, T.G. Langdon, Mater. Sci. Eng. A 347 (2003) 223.
- [25] S. Qu, C.X. Huang, Y.L. Gao, G. Yang, S.D. Wu, Q.S. Zang, Z.F. Zhang, Mater. Sci. Eng. A 475 (2008) 207.
- [26] J. May, H.W. Höppel, M. Göken, Scripta Mater. 53 (2005) 189.
- [27] Y.G. Ko, D.H. Shin, K.T. Park, C.S. Lee, Scripta Mater. 54 (2006) 1785.
- [28] M.L. Wang, A.D. Shan, J. Alloys Compd. 455 (2008) L10.
- [29] Z.F. Zhang, J. Eckert, Phys. Rev. Lett. 94 (2005) 094301.
- [30] J.K. Kim, H.J. Jeong, S.I. Hong, Y.S. Kim, W.J. Kim, Scripta Mater. 45 (2001) 901.
- [31] P.L. Sun, C.Y. Yu, P.W. Kao, C.P. Chang, Scripta Mater. 47 (2002) 377.
- [32] B.Q. Han, J.Y. Huang, Y.T. Zhu, E.J. Lavernia, Scripta Mater. 54 (2006) 1175.
- [33] T.H. Courtney, Mechanical Behavior of Materials, The McGraw-Hill Companies, 2000, pp. 149–152.
- [34] Y. Fukuda, K. Oh-ishi, M. Furukawa, Z. Horita, T.G. Langdon, Acta Mater. 52 (2004) 1387.
- [35] D.C. Drucker, Metall. Trans. 4 (1973) 667.